The Fibrillar Structure of Cellulosic Man-Made Fibers Spun from Different Solvent Systems*

J. LENZ, *Lenzing AG, A-4860 Lenzing, Austria,* and J. SCHURZ and E. WRENTSCHUR, *Institut für Physikalische Chemie der Universität Graz, Heinrichstrasse 28, A-8010 Graz, Austria*

Synopsis

The development of new methods of spinning cellulosic fibers requires a better understanding of their fibrillar structure in order to explain their special physical properties. By means of transmission electron microscopy (TEM), light microscopy (LM), small-angle X-ray scattering (SAXS), and wide-angle X-ray diffraction (WAXD) it is shown that six different kinds of regenerated cellulosic fibers consist of uniform elementary fibrils composed of cellulose-II crystals. Systematic distinctions between these fiber types are found with regard to the aggregation of the elementary fibrils to nonswelling bundles or clusters. The clusters differ from each other in diameter, length, and frequency of occurrence.

INTRODUCTION

Frey-Wyssling was the first who suggested that the microfibrils of natural occurring cellulose I were the product of fasciation of crystalline smaller threads, to which he gave the name of "elementary fibrils." They should have the shape of long ribbonlike strings with a cross section of approximately 3×7 nm. The strings were held together by amorphous material to form the whole microfibril.[1] Preston, however, concluded that these results, found by means of TEM, are artifacts with respect to the existence of elementary fibrils.[2] Sullivan observed that the diameters of the so-called elementary fibrils are dependent on the time the material was subjected to the ultrasonic treatment.[3] Heyn was the first to apply the preparation technique of negative staining to the electron-microscopic study of the fibrillar structure of natural cellulose fibers.[4] Unlike the metal shadowing, staining is carried out in the uncollapsed, water-swollen state, in which the staining solution penetrates between the fibrils and is deposited there upon drying. Therefore, conglomeration and collapsing to artifacts during drying may be largely prevented. Heyn detected beaded appearing elementary fibrils with a periodic change of crystallinity. The crystals were clearly visible, because only the amorphous portions take up the stain, the crystalline portions remaining unstained. Preston's criticism of this method is based on the assumption that the fibrils have a circular cross-section; in fact, it is rectangular.

*Paper presented on occasion of the International Dissolving Pulps Conference, March 24–27, 1987, in Geneva, Switzerland.

Journal of Applied Polymer Science, Vol. 35, 1987–2000 (1988)
 CCC 0021-8995/88/081987-14$04.00

Apart from natural cellulose fibers regenerated cellulosic fibers were studied using hydrolysis, ultrasonic treatment, and metal shadowing by Dlugosz and Michie,[5] Mühlethaler,[6] Takai et al.,[7] Ribi,[8] and Mukherjee et al.[9] Schurz and John used jodination according to Hess and detected in fibrils of Fortisan a periodicity in the order of the long period.[10] Manley[11] again used the negative staining technique. In Fortisan he detected thin parallel filaments about 3 nm in width, which looked like beadchains similar to the fibrils found by Heyn.[11] Lenz et al. found in hydrolyzed viscose fibers chains of platelets, the dimensions of which were consistent with the wide- and small-angle X-ray data.[12] Nevertheless, the existence of elementary fibrils is still controversial today.

In contrast to natural cellulose fibers, there is till now no evidence for the existence of microfibrils in man-made cellulosic fibers.

EXPERIMENTAL

Fiber Samples

NMMOs 1 and 2 are fibers spun from a solution of cellulose in *N*-methylmorpholineoxidehydrate (Akzona). DMAc/LiCl 1, 2, and 3 are fibers spun from a solution of cellulose in dimethylacetamide/lithiumchloride (laboratory). Carbamates 1 and 2 are fibers spun from a solution of cellulose carbamate in sodium lye (Neste OY). Modal is a high wet modulus fiber (Lenzing AG). Polynosic is polynosic fiber (Toyobo). Viscose 1 is a viscose fiber (Lenzing AG), and viscose 2 is a high tenacity viscose fiber (Lenzing AG).

Preparation of Samples

For X-ray examinations the fiber samples were hydrolyzed 24 h at 60°C in 1*N* HCl, washed and dried. The weight loss varied from 2.5% (Polynosic) to 7% (modal). After this treatment a level-off DP of 130 was determined. For transmission electron microscopy the samples were hydrolyzed 48 h and subsequently ultrasonified for 15–60 min.

Determination of the Long Period by Means of SAXS

The specimens were subjected to X-ray examination in their original fibrous form. The X-ray scattering curves were obtained by means of a Kratky camera equipped with a slitfocus. The width of the entry slit was 60 μm, the width of the counting tube slit 150 μm. An X-ray tube with Cu target and Ni filter was run with a commercial X-ray unit. The long period could be obtained clearly from the line profiles at 2θ of maximum peak.

Bragg's equation was used for the calculation of the long period

$$2d \sin \theta = n \cdot \lambda \tag{1}$$

where d is the period of identity of the electron density fluctuation along the fiber axis, n is an integer, θ is half the scattering angle, and λ is the wavelength (Cu K_α: 0.15418 nm).

Determination of the Lateral Period of Identity by Means of SAXS

The same technique was used as described above with the difference that the fiber specimen was arranged in the camera horizontally instead of vertically. For the X-ray examination of the fibers in the swollen state the specimen containing the glass tube was connected by a flexible pipe with a

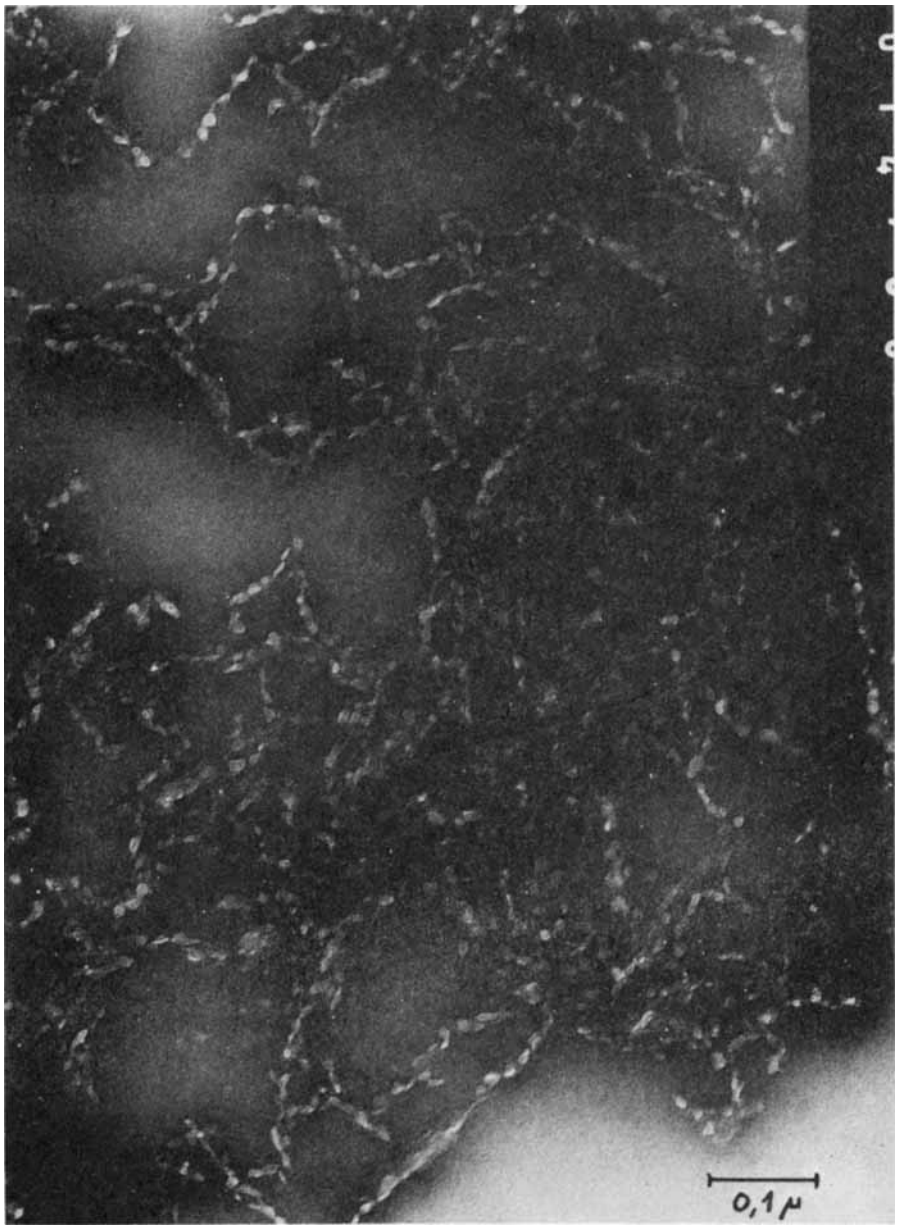

Fig. 1. Transmission electron micrograph of a hydrolyzed, disintegrated modal-fiber (magnification 204,000×, hydrolyzing time 50 h, ultrasonic treatment 15 min).

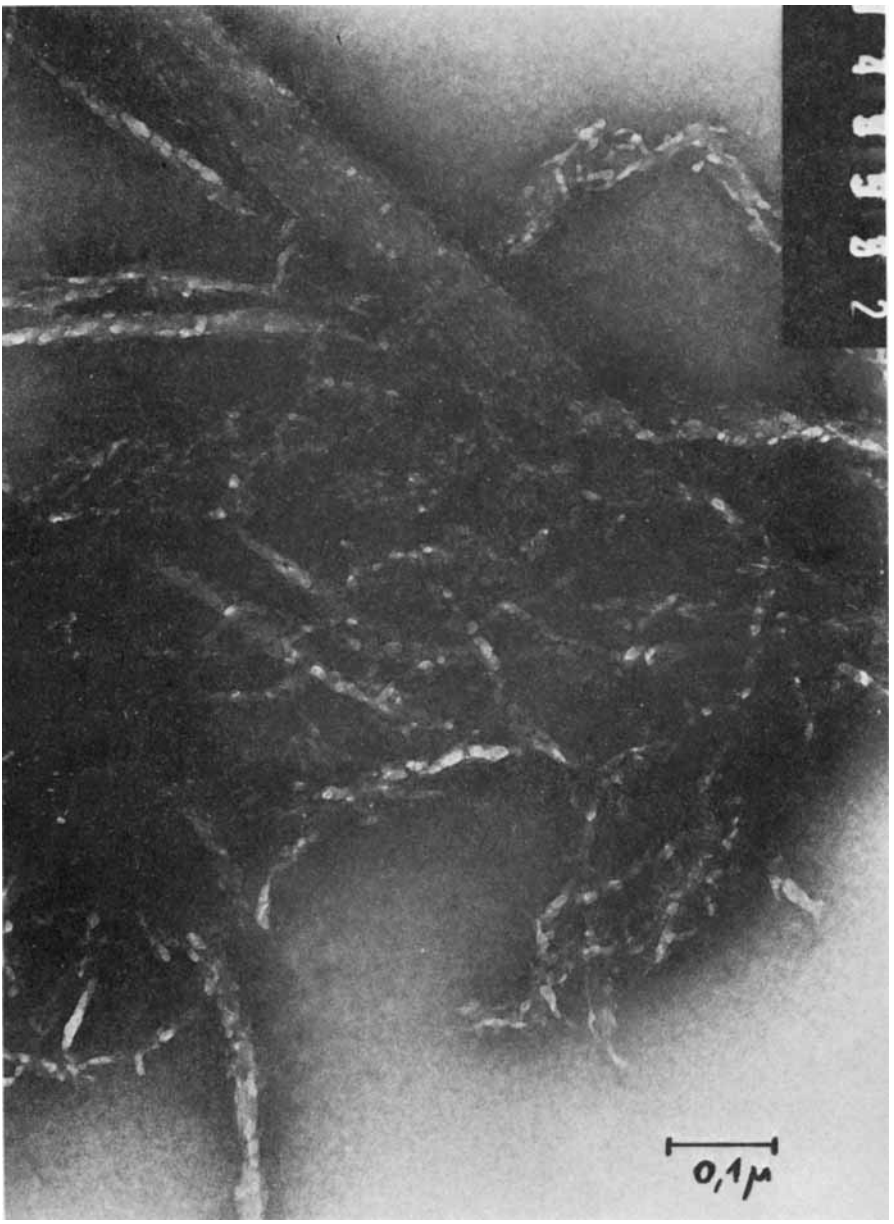

Fig. 2. Transmission electron micrograph of a hydrolyzed, disintegrated fiber, spun from a solution of cellulose in dimethylacetamide/LiCl (magnification 204,000×, hydrolyzing time 60 h, ultrasonic treatment 20 min).

water reservoir. In the equation d means the period of identity normal to the fiber axis.

Determination of the Degree of Crystallinity and the Orientation Factor by Means of WAXD

The degree of crystallinity was determined by means of planimetry of the equatorial wide-angle X-ray diffractograms. The curve for the elimination of the background was drawn visually. From the azimuthal intensity distribution of the well-resolved wide-angle X-ray reflection lines 101 and $10\bar{1}$, the orientation factor was calculated according to Kratky.[15]

Determination of the Size of Crystallites and Clusters by Means of TEM

After a hydrolyzing time of 48 h in 1N HCl at 60°C the fibers were found to be destroyed. In some cases hydrolyzing had to be prolonged for 100 h. Afterward the fibril suspension was further disintegrated by means of a Bronson Sonifier 830 at 150 W and 20 Hz. The applied times of hydrolyzing and sonifying did not change the dimensions of the crystallites. The material was prepared for TEM according to the method of negative staining with phosphotungstic acid. It is assumed, that the amorphous portions take up the stain, whereas the crystalline portions remain unstained (Figs. 1 and 2). On each electron micrograph we measured the maximum length, width, and thickness of each well visible oval shaped platelet. Each given value is the average of 80 measurements. Moreover, we measured both length and diameter of each bundle of elementary fibrils.

Determination of the Degree of Swelling by Means of LM

The diameter of the weakly hydrolyzed fibers was measured by means of a measuring ocular as well in the dry as in the wet state, i.e., immersed in water. Each value is the average of 20 measurements.

RESULTS AND DISCUSSION

The electron micrographs of the hydrolyzed fibers show strings of platelets, which occur either isolated (Fig. 1) or aggregated to bundles (Fig. 2). If these strings are identical with elementary fibrils, the platelets must be cellulose-II crystals. In order to identify these morphological units, we measured the long periods of the corresponding weakly hydrolyzed fiber samples being aware of the fact that acidic hydrolysis increases the original crystal size.

In Table I the following data are put together: the average length of the platelets, the long period, the degree of crystallinity, and the crystalline orientation factor. As is to be seen, the long periods are 30–40% larger than the lengths of the platelets. This is due to the fact that the long period covers the length of a whole period of electron density fluctuation including the less ordered interspace between two crystallites. From the rather constant ratio between the length of the platelets and the long period we conclude that the platelets are in fact cellulose-II crystals. If this is true, the beaded chains on the electron micrographs must be elementary fibrils.

TABLE I
Summary of the Fine Structural Data of All Investigated Fiber Samples

Fiber	TEM, length of the platelets (nm)	SAXS, long period (nm)	WAXD	
			Crystallinity (%)	Orientation factor fr
NMMO 1	14.4	18.7	54.8	0.60
NMMO 2	16.0	22.0	59.5	0.80
Carbamate 1	—	17.9	50.6	0.67
Carbamate 2	12.3	16.6	50.1	0.71
DMAc/LiCl 1	12.9	18.2	31.3	0.28
DMAc/LiCl 2	13.0	—	31.0	0.26
DMAc/LiCl 3	16.5	17.9	33.1	0.67
Modal	13.2	17.2	47.0	0.53
Polynosic	13.9	17.4	48.3	0.54
Viscose 1	10.0	14.3	33.0	0.36
Viscose 2	11.0	14.3	34.7	0.39

If cellulosic fibers consist of regularly shaped fibrils, the latter must be detectable also by measuring the equatorial SAXS curve, because their existence would implicate electron density fluctuations normal to the fiber axis. In 1953 Hermans and co-workers already discovered in the equatorial SAXS curves of certain regenerated cellulose fibers a small inflection or bulge, caused by a superimposed interference maximum, which he supposed to be an indication of the presence of uniform, lamella-like particles packed in a regular manner.[13] From the scattering angle, at which the inflection appears, he calculated a lateral period of identity using eq. (1). He found 4.5–5.5 nm for dry fibers and 7.0–8.5 nm for water-swollen fibers. Heyn made similar observations.[14]

Because the monoaxially oriented fibers are arranged parallel to the streak-like focus of the Kratky camera; the effect of the Lorentz factor of the lamella length and the smearing of the gap neutralize each other. For this reason the Lorentz factor must not be eliminated from the scattering curves. That means according to Kratky that the position of the superimposed interference maximum of the equatorial SAXS curve is a useful measure for the upper limit of the width of a lamella.[15] So the occurrence of an interference maximum in the equatorial SAXS curve is an indication that the scattering particles must be lamella-shaped bodies ordered parallel to each other. This picture would be consistent with the existence of ribbonlike elementary fibrils.

Following up these considerations, we measured the equatorial SAXS curves of the fiber samples in the dry and water-swollen state. Two examples are shown in Figures 3 and 4. In conformity with Hermans' results the dry fibers show a weak inflection at a period of identity of 6–7 nm, whereas the wet fibers show a strong interference maximum at a lateral period between 9 and 18 nm. In Table II, columns 1 and 2, the results are listed.

The question arises why the inflections in the wet state are more distinct and correspond to a larger lateral period. In this respect one has to realize that the basic equatorial SAXS curve of a dry cellulose fiber is caused by pores of collodial dimensions.[16] Through swelling of the fibers in water, these voids will be filled, causing a sharper appearance of the interference maxi-

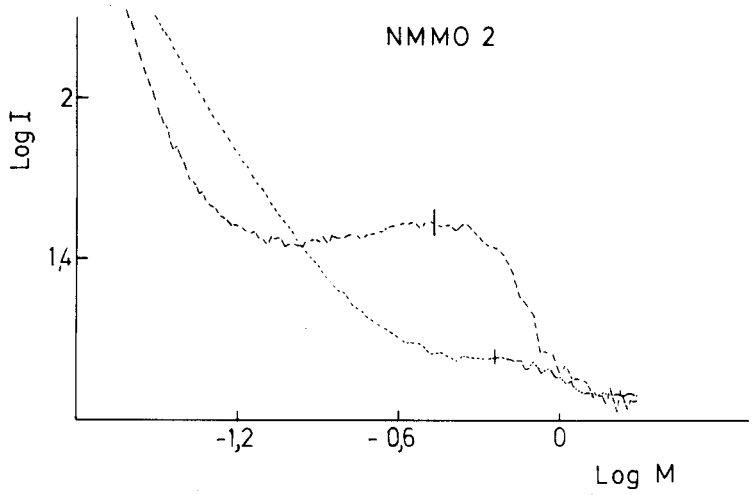

Fig. 3. Equatorial SAXS curve of a fiber, spun from a solution of cellulose in *N*-methylmorpholineoxidehydrate: (· · ·) dry state; (- - -) wet state. M = scattering angle as distance from the center of the primary beam; I = X-ray scattering intensity.

mum. In addition, the particles will be separated from each other by swollen less-ordered cellulose, giving rise to a larger period of identity normal to the fiber axis.

Columns 4 and 5 of Table II show width and thickness of the cellulose-II crystals measured by means of TEM. The average thickness of the crystals of 2.5–3 nm amounts approximately to 40% of the lateral period in the dry state in the range of 6.0–7.0 nm. As the crystals are covered with less-ordered cellulose, one has to expect a difference between the thickness of the crystals and the lateral period in the order of the crystallinity. The latter ranges between 30 and 60% according to Table I, column 3.

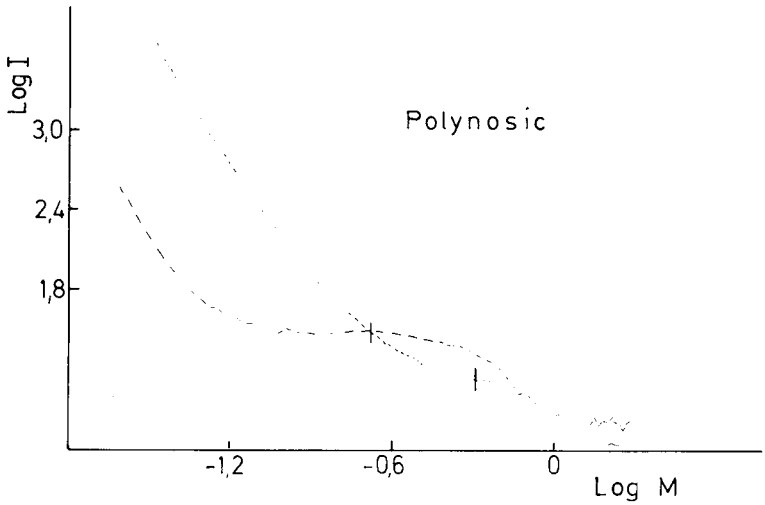

Fig. 4. Equatorial SAXS curve of a polynosic fiber.

TABLE II
Internal and Macroscopic Swelling of the Fiber Samples

Fiber	SAXS, lateral period			TEM: Width Thickness of crystals		LM, macroscopic swelling	Cluster
	Dry (nm)	Wet (nm)	Increase (degree)	(nm)	(nm)	(degree)	fraction
NMMO 1	6.0	12.4	2.06	7.1	2.5	1.66	0.38
NMMO 2	6.9	9.1	1.32	6.2	2.6	1.23	0.28
Carbamate 1	6.7	12.9	1.93	—	—	—	—
Carbamate 2	6.1	16.6	2.70	8.8	2.6	—	—
DMAc/LiCl 1	6.5	18.2	2.78	7.9	2.6	1.27	0.85
Modal 1	7.0	13.8	1.97	8.7	3.1	1.13	0.87
Polynosic	6.4	15.5	2.44	7.6	2.5	1.34	0.76
Viscose 1	6.5	18.5	2.86	6.3	2.4	1.31	0.83
Viscose 2	6.6	18.4	2.79	5.1	1.9	1.23	0.87

In contrast to the dry state the lateral periods in the swollen state differ strongly from each other. The increase of the lateral period by water swelling varies between 30 and 180%. That means that the less-ordered cellulose between the crystals must take up different amounts of water. This conclusion will be supported by the fact that the increase of the lateral period by swelling correlates in inverse proportion with the crystalline orientation factor, as is shown in Figure 5.

In comparison with the internal degree of swelling, the macroscopic degree of swelling was also determined by light microscopical observation of the increase of the thickness of the in-water immersed fibers. The results are given in column 6 of Table II. Comparing the internal with the macroscopic degree of swelling, it becomes evident that the latter is much less than the former. That means that a certain portion of the fiber substance does not swell in water.

In so-called air-swollen cellulose, which is swollen and subsequently porously dried viscose fiber, Kratky found a portion of the material being present in the form of large, dense particles or clusters of cellulose crystals.[17] Assuming that in water-swollen fibers such nonswollen clusters may occur, too, the degree of the supposed cluster formation of the different fiber samples was calculated from the internal and macroscopic degree of swelling using the following equation given by Kratky and Miholic:[17]

$$f = (q - q')/(1 - q') \tag{2}$$

where f means the cluster fraction, q the macroscopic degree of swelling, and q' the internal degree of swelling. The portions of the assumed cluster fraction are listed in the last column of Table II. The values are astonishingly high.

The assumption of the existence of nonswelling bundles of elementary fibrils is supported by the transmission electron micrographs. They show such bundles, which obviously did not swell during hydrolysis, ultrasonic treatment, and staining even after very prolonged treatments.

Because a morphological observation is no proof, showing the existence of nonswelling clusters was tried by measuring the equatorial SAXS curves of

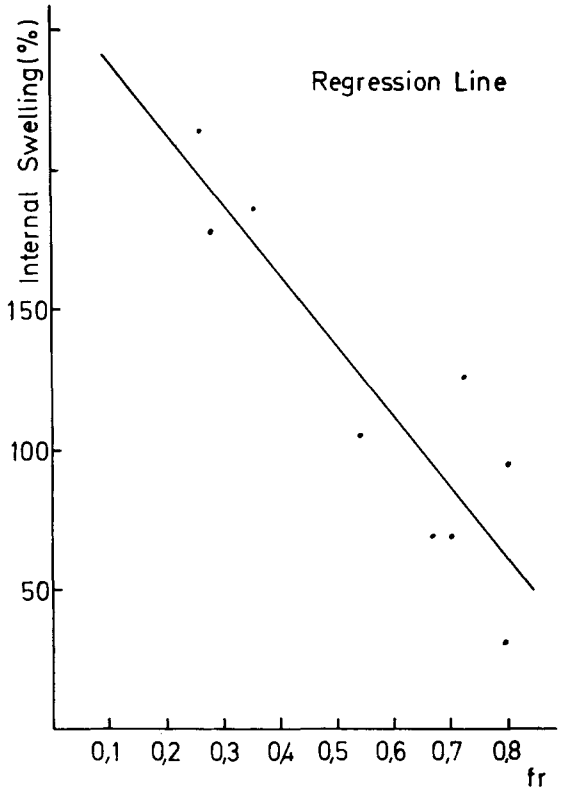

Fig. 5. Correlation between the internal swelling and the orientation factor (fr): coefficient of correlation −0.894; statistical confidence 99.9%.

the weakly hydrolyzed water-swollen fibers at extremely small angles according to Guinier's theory of particle scattering. Infinitely diluted particles of collodial dimensions give rise to an X-ray scattering curve, which in the Guinier plot, i.e., the logarithm of the scattering intensity vs. the square of the scattering angle, approaches with decreasing scattering angle to a straight line.[18] In a monoaxially oriented, monodisperse system the limiting slope of the Guinier curve is a function of the radius of gyration of the cross section of the scattering particles. Assuming a circular cross section of the elongated scattering particles, infinite length with respect to the wavelength, and parallel orientation, one can calculate the cluster diameter according to the following equations:[19,20]

$$Rq = 0.526 \cdot a \cdot \sqrt{tg\alpha} \tag{3}$$

$$Rq^2 = r^2/2 \tag{4}$$

where Rq means the radius of gyration of the cross section, α the slope of the curve of log I vs M^2, r the radius of the cylindrical particle, a the distance between sample and counting tube, I the scattering intensity, and M the scattering angle as distance from the center of the primary beam. If, however,

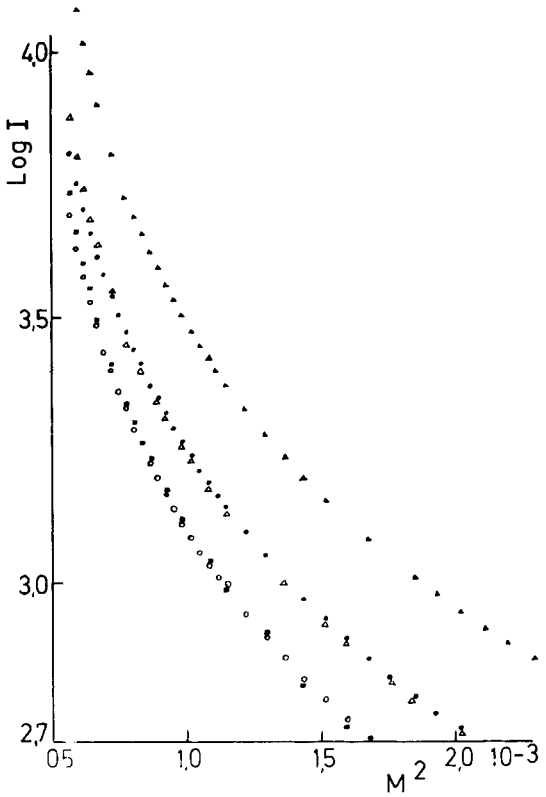

Fig. 6. Equatorial SAXS curves of different cellulosic fibers in Guinier plot in dry state: (●) NMMO 2; (○) modal 1; (△) viscose 1; (■) DMAc/LiCl 1; (▲) carbamat 1.

the Guinier plot has a curvature convex in relation to the ordinates, the particles do not scatter independently from each other, because of interference effects.

Figure 6 shows the Guinier plot of the fiber samples in the dry state. Obviously the inner part of the curves does not run out into a straight line approaching the scattering angle zero. This is due to the fact that the dry fiber is a densely packed system in which interparticle interference effects are dominant. Particle scattering occurs only in very porous fibers, such as air-swollen, viscose fibers[17] or porous polyacrylonitrile fibers.[19]

Figure 7 represents SAXS curves in the Guinier plot, which were obtained by exposing the immersed, swollen fibers to X-ray examination. Under these conditions the curves show straight-lined sections with distinct slopes. This curvature can be interpreted as the superposition of different Guinier scattering curves of a polydisperse system. Bearing in mind that the scattering of open pores in swollen fibers has to be neglected, this scattering must be due to dense particles of different diameter distributed in a matrix of water-swollen cellulose. Two kinds of fibers show a different curvature, as is seen in Figure 8, namely modal and carbamate fibers. Again these curves are convex in relation to the ordinates. Evidently in these fibers the clusters do not scatter independently from each other. However, these curves also run out into a straight

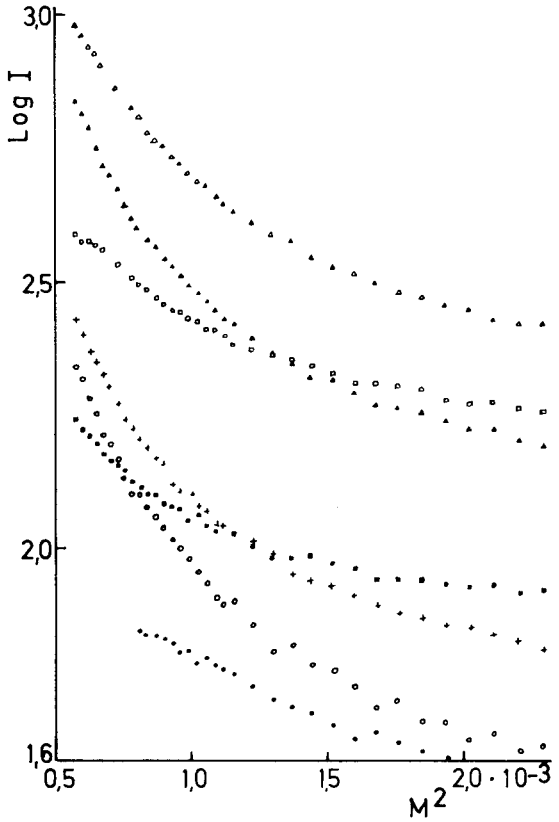

Fig. 7. Equatorial SAXS curves of different cellulosic fibers in a Guinier plot in a water-swollen state: (●) NMMO 1; (○) NMMO 2; (■) DMAc/LiCl 2; (□) DMAc/LiCl 1; (+) DMAc/LiCl 3; (△) viscose 1; (▲) modal 3.

line, which in the direction of increasing scattering angles turns into the interference maximum of the elementary fibrils.

An attempt was made to calculate the cluster diameters from the slopes of the straight-lined curve sections. As the measured curves are the result of a superposition of different scattering curves, corresponding to different cluster sizes, the latter would have to be separated before the evaluation. Regarding the short length of the straight-lined sections this would be problematic. Therefore, only the outmost curve sections having the lowest slope were evaluated assuming that this part of the SAXS curve is caused by only one particle size. As the sections are rather short, one has to bear in mind that the calculated values correspond to the lower limit of the cluster diameter.

Table III shows the cluster diameters, calculated from the straight-lined curve section, which has the lowest slope, using the eqs. (3) and (4). Comparing these values with the average diameters of the bundles of elementary fibrils, which were gained by evaluation of the TEM micrographs, a certain conformity can be noticed. At each sample the cluster diameter calculated from the SAXS curves lies within the variation of the average diameter of the bundles measured on the micrographs.

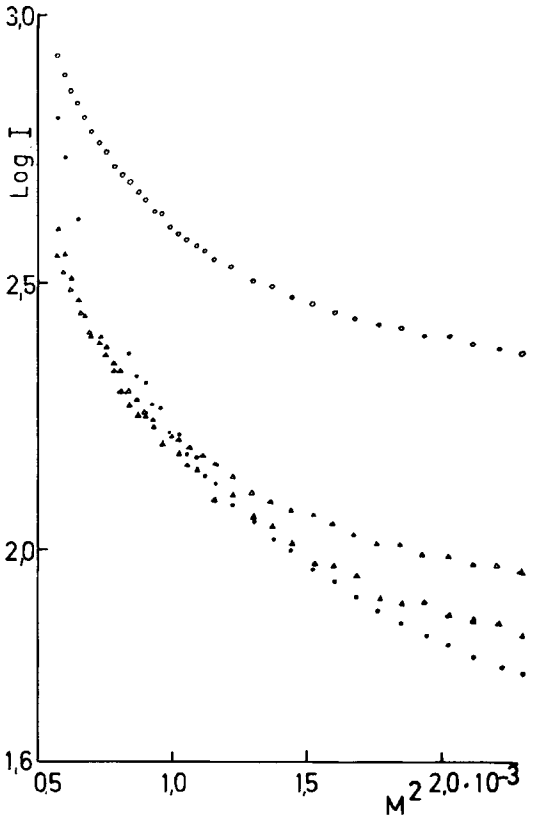

Fig. 8. Equatorial SAXS curves of differentcellulosic fibers in a Guinier plot in a water-swollen state: (●) carbamat 1; (○) carbamat 2; (▲) modal 1; (△)modal 2.

TABLE III
Dimensions of the Clusters by TEM and SAXS

Fiber	Cluster diameter			Cluster length, TEM (nm)
	SAXS (nm)	TEM (nm)	TEM (SD)	
NMMO 1	50.6	36.5	18.1	289
NMMO 2	51.7	47.0	—	243
Carbamate 2	32.3	54.0	—	> 400
DMAc/LiCl 1	28.6	40.7	17.6	> 400
DMAc/LiCl 2	28.2	40.7	17.6	> 400
DMAc/LiCl 3	37.7	44.6	22.1	> 400
Modal 1	33.7	39.4	18.1	184
Polynosic	51.5	35.9	—	188
Viscose 1	48.3	49.0	13.0	150
Viscose 2	30.8	43.2	17.4	144

In the fourth column of Table III the lengths of the clusters taken from the TEM micrographs are put together. Comparing these values, one notices great distinctions between the different fiber samples. In the cases of the DMAc/LiCl and carbamate fibers,the cluster lengths are larger than 400 nm, as at the other kinds of fibers the clusters are as short as 150–240 nm. Possibly the clusters of distinct fiber types are different stable against the ultrasonic treatment. Supposedly, one observes only fragments of the original clusters on the micrographs of the disintegrated fiber samples.

CONCLUSION

The results show that all investigated kinds of fibers spun from different solvent systems consist of uniform elementary fibrils. In contrast to this result, there are systematic distinctions between the different fiber types regarding the aggregation of the elementary fibrils to nonswelling clusters.

Table II shows that fibers spun from a solution of cellulose in *N*-methylmorpholineoxide hydrate exhibit the lowest cluster fraction. Regarding Table III, it is remarkable that the cluster lengths harmonize within certain fiber types. Obviously the cluster length increases in the following order: normal viscose fibers, high wet modulus fibers, *N*-methylmorpholineoxide fibers, and fibers spun from a solution of cellulose in dimethylacetamide/lithiumchloride, respectively, from a solution of cellulose carbamate in sodium lye. It should be mentioned that the corresponding elongations at break decrease in the same sequence, if the fibers are oriented during their production to the maximum: normal viscose fibers 16–17%, high wet modulus fibers 11–14%, *N*-methylmorpholineoxide fibers 11%, and dimethylacetamide/lithiumchloride fibers 6–8%. Carbamate fibers make an exception with an elongation at break of 11–13%.

So it seems that the formation of very stable, long bundles of elementary fibrils reduces the elongation at break at a given orientation. This assumption is reasonable because the rupture of a fiber during stretching is the result of microstresses, which are more likely in the presence of rigid bodies being unable to comply with the external tension.

We thank Dr. W. Geymayer for making the electron micrographs.

References

1. A. Frey-Wyssling, *Science*, **119**, 80 (1954).
2. J. Nieduszynski and R. D. Preston, *Nature*, **225**, 273 (1970).
3. J. D. Sullivan, *Tappi*, **51**, 501 (1968).
4. A. N. J. Heyn, *J. Cell. Biol.*, **20**, 182 (1966).
5. J. Dlugosz and R. I. C. Michie, *Polymer*, **1**, 41 (1960).
6. K. Mühlethaler, *Experientia*, **VI / 6**, 226 (1949).
7. M. Takai, K. Kohno, and I. Hayashi, *Cell. Chem. Technol.*, **18**, 447 (1984).
8. E. Ribi, *Ark. Kemi. Mineral. Geol.*, **2**, 551 (1950).
9. S. M. Mukherjee, S. Sikorski, and H. J. Woods, *J. Text. Inst.*, **43**, 196 (1952).
10. J. Schurz and K. John, *Cell. Chem. Technol.*, **9**, 493 (1975).
11. J. Manley, *J. Polym. Sci., Part A-2*, **9**, 1025 (1971).
12. J. Lenz, J. Schurz, E. Wrentschur, and W. Geymayer, *Angew. Macromol. Chem.*, **138**, 1–9 (1986).
13. D. Heikens, P. H. Hermans, P. F. van Velden, and A. Weidinger, *J. Polym. Sci.*, **11**, 433 (1953).

14. A. N. J. Heyn, *Nature*, **172**, 1000 (1953).
15. O. Kratky and G. Porod, *Die Physik der Hochpolymeren*, H. A. Stuart, Ed., Springer-Verlag, Berlin, 1955, Vol. 3.
16. W. O. Statton, *J. Polym. Sci.*, **22**, 385 (1956).
17. O. Kratky and G. Miholic, *J. Polym. Sci., Part C, No. 2*, 449 (1963).
18. O. Kratky, *X-Ray Small-Angle Scattering with Substances of Biological Interest in Diluted Solutions*, Pergamon, New York, 1963, reprinted from *Progress in Biophysics*, Vol. 13.
19. J. Schurz, H. Janosi, E. Wrentschur, H. Krässig, and H. Schmidt, *Colloid Polym. Sci.*, **260**, 205 (1982).
20. P. Mittelbach, *Acta Physica Austr.*, **19**(1), 53 (1964).

Received September 15, 1987
Accepted September 21, 1987